HHS Public Access

Author manuscript

J Am Chem Soc. Author manuscript; available in PMC 2021 April 06.

Published in final edited form as:

J Am Chem Soc. 2020 May 20; 142(20): 9240–9249. doi:10.1021/jacs.9b12898.

Optical manipulation of F-actin with photoswitchable small molecules

Malgorzata Borowiak[1,#], **Florian Küllmer**[2,#], **Florian Gegenfurtner**[1], **Sebastian Peil**[2], **Veselin Nasufovic**[2], **Stefan Zahler**[1], **Oliver Thorn-Seshold**[1], **Dirk Trauner**[3,*], **Hans-Dieter Arndt**[2,*]

[1]Department of Pharmacy, Ludwig-Maximilians University, Butenandtstrasse 5-13, D-81377 München, Germany

[2]Institute for Organic Chemistry and Macromolecular Chemistry, Friedrich-Schiller-University, Humboldtstrasse 10, D-07743 Jena, Germany

[3]Department of Chemistry, New York University, 100 Washington Square East, New York, NY 10003, USA.

Abstract

The spatiotemporally-controlled perturbation of cellular function using photopharmacology has facilitated the elucidation of biological networks and opens up new opportunities for precision medicine. Here, we introduce cell- permeable photoswitchable small molecules, termed **optojasps**, to optically control the dynamics of the actin cytoskeleton and cellular functions that depend on it. These light-dependent effectors were designed from the F-actin-stabilizing marine depsipeptide jasplakinolide by functionalizing them with azobenzene photoswitches. We demonstrate that **optojasps** can be employed to control cell viability, cell motility, and cytoskeletal signalling with the high spatial and temporal resolution that light affords. We expect that **optojasps** will find applications in diverse areas of cell biological research. They may also provide a template for the development of chemotherapeutics targeting the ubiquitous actin cytoskeleton with precision control in the μm range.

Graphics for the table of contents

[*]*Corresponding authors* hd.arndt@uni-jena.de, dirktrauner@nyu.edu.
[#]These authors contributed equally

Associated Content

Supporting Information

The supporting information is available free of charge at https://pubs.acs.org/… Enclosed are supporting figures for MTT assays (figure S1), binding pocket region in F-actin (figure S2), extended photoswitching stability trace of optojasp1 (figure S3), raw data of F-actin polymerization experiments (figure S4) and isomerization stability monitoring (figure S5), Materials and Methods including solubility and aggregation data (supporting tables S1 and S2), Chemical Synthesis and Characterization, Optojasp HPLC traces (figure S4), ^{1}H-NMR spectra, UV-Vis spectra (figure S6, one composite PDF file), as well as supplementary video material (additional AVI files).

Notes

The authors declare no competing financial interests. Correspondence and requests for materials should be addressed to H.-D.A. and D.T.

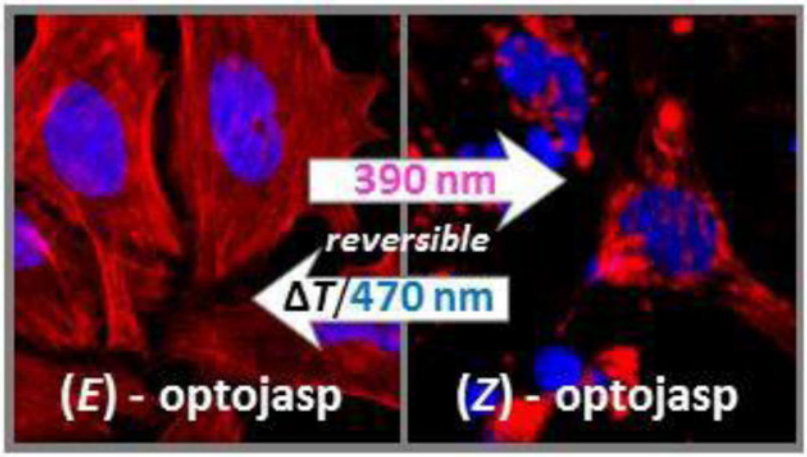

Introduction

Actin is the most abundant cellular protein and an essential component of the eukaryotic cytoskeleton.[1] Its ability to reversibly assemble into long supramolecular filaments[2] drives the definition of cell shape, migration, endocytosis, phagocytosis, and intracellular transport. In neurons, actin remodeling configures dendritic spines, is required for synapse function, and is a key component in axonal growth.[3] In the nucleus, nuclear actin contributes to RNA transcription and chromatin maintenance.[4] Actin also plays a critical role in cell division as an essential component during cytokinesis.[5]

The actin cytoskeleton is highly dynamic and undergoes constant remodeling in response to the physiological state and external stimuli. From a pool of a globular monomeric form (G-actin), a polymeric, filamentous form (F- actin) is generated, which dynamically interconverts through assembly and disassembly in an ATP-dependent and consuming process (“treadmilling”). F-actin consist of two helically intertwined strands of a supramolecular protein polymer fiber that can be hierarchically arranged by actin binding proteins in parallel bundles, branched dendritic networks and stress fibers, leading to diverse microfilament topologies and dynamics.[1]

The key role of actin dynamics in living organisms has led to the evolution of interfering secondary metabolites,[6] including the polyketides cytochalasin[7] and latrunculin,[8] as well as the (bi)cyclic peptides phalloidin (**1**), chondramide (**2**), and jasplakinolide (**3**, sometimes also referred to as “jaspamide”, Fig. 1a).[9] The cytochalasins and the latrunculins retard polymerization and enhance depolymerization by binding tightly to the G-actin monomer.[10] By contrast, phalloidin and jasplakinolide are incorporated at the interface between three actin subunits, promoting aggregation, and suppressing depolymerization.[11] These small molecules and their derivatives have become powerful tool compounds for research.[12,13] Fluorescent derivatives of phalloidin are common reagents for visualizing actin filaments in fixed cell microscopy.[14] The silicon- rhodamine derivative **4** of jasplakinolide, termed SiR-actin, is cell permeable and images F-actin dynamics in living cells.[15] SiR-actin is prepared

by total synthesis and features an optimized jasplakinolide-derived structure[16] that is more chemically stable (Fig 1b).

Although actin inhibitors have potent anti-migratory activity and are toxic to cancer cells, systemic toxicity resulting from disturbed actin dynamics in healthy tissue has prevented them from reaching therapeutic application.[17] Moreover, many actin-dependent processes are anisotropic and time-dependent,[18,19] which limits the utility of globally-acting inhibitors.[6,12] Inhibitors that could instead be directed to modulate the actin cytoskeleton more precisely would circumvent these drawbacks and be extremely valuable for research and therapy.

Spatiotemporal control can be realized by incorporating photoswitches into bioactive molecules.[20,21] Molecular photoswitches are particularly well suited to modulate dynamic, non-linear processes, as featured in cytoskeleton biology, in G-protein coupled receptor pathways, and in neuronal signalling. Indeed, photopharmacology has been successfully used *in vivo* to control receptor signalling,[22] tubulin dynamics,[23] and to restore visually guided behaviour in blind animals.[24] Azobenzenes that show metastable irradiation-dependent change in their diazene configuration have been frequently applied in this regard (Fig 1C).[24,25] Here, we introduce a family of azobenzene-based small molecules, termed **optojasps**, that provide direct optical control of the actin cytoskeleton.

Design and Synthesis of the Optojasps

For designing the **optojasps**, the noticeable dependence of cell permeability and actin-staining potential on fluorophore type and linker length of conjugates, such as **4,** was key.[15,16] Without any specific mechanistic conjecture, it suggested that modulating the activity of jasplakinolides by placing an azobenzene in the same region as the fluorophore of **4** might be possible. Such an “azo-extension” strategy has been successful with ion channel blockers[26] and dihydrofolate reductase inhibitors.[27] For initial screening, a panel of eight **optojasps** was considered, which differed in the length of the connecting amino acid side chain (diaminopropionate, diaminobutyrate, ornithine, lysine) and in the geometry of the appended azobenzene photoswitch (Fig. 2A). The latter were connected in *para* (azo-1, Fig 2C) or *ortho* (azo-2) in order to probe for different interactions exerted by the photoswitch in its respective *trans* and *cis* isomeric states.

The azobenzenes finally chosen featured 4,4’-dialkoxy substituents to ensure high bidirectional completion of photoswitching and retarded thermal isomerization. They were 3,4,5-trimethoxylated in the A-ring to improve solubility by disfavouring compound aggregation (Fig. 2A and C).[23] Notably, while structurally related photostatin switches (e.g. **18**, Fig 2C) have been successfully used for targeting tubulin,[23] extensive SAR studies and successful prodrug designs of combretastatin analogs[28] as well as recent high-resolution X-ray crystal structures of tubulin-bound combretastatin in *cis*- and *trans*-configuration[29] suggested that any protrusion from the B-ring significantly larger than the *para* methoxy group of azobenzene **18** (Fig 2C, highlighted) entirely abrogates affinity for tubulin. Therefore, “clean” actin-selective photoswitches were expected to result from conjugation of the extended azo-1 (**16**) or azo-2 (**17**) scaffolds.

The syntheses of **optojasps** then used six building blocks each (Fig. 2C).[15,16,30] In brief, β-tyrosine derivative **5** was immobilized on solid phase (**6**, Fig. 2B) and was sequentially extended by solid phase peptide synthesis (SPPS) with *N*-Me-Trp building block **11**, one of the diamino building blocks **12a-d**, and the unsaturated acid **13**, to give tripeptides **7a-d** after cleavage from the resin. Esterification with alcohol **14** provided dienes **8a-d**. Ring closing metathesis with Grubbs' 2nd generation catalyst **15** yielded the macrocyclic cyclodepsipeptides **9a-d** as *E*- configured cycloalkenes. After acid-mediated deprotection, the ammonium salts **10a-d** were coupled to azobenzene carboxylic acids azo-1 (**16**) or azo-2 (**17**) and deprotected to afford **optojasps1–8** (Fig. 2b) in 10–20% overall yield.

Photochemical and Biological Evaluation

An initial evaluation of the photochemical properties of **optojasps-1−8** showed that all compounds were photoswitched *trans*→*cis* with deep violet and *cis*→*trans* with green light, reaching satisfactory photostationary ratios upon deep violet irradiation (*cis*/*trans* typically 10:1). They were fairly thermally stable to spontaneous *cis*→*trans* relaxation (Fig. 3). The **azo-1** derived photoswitches showed very slow thermal relaxation ($t_{1/2}$ ~ 36 h), whereas **azo-2** switches displayed a relaxation half-life of ~80 min in CH_3CN at 25°C. Not unexpectedly, thermal relaxation was found accelerated under physiologically relevant conditions (37°C, determined in aqueous buffer, see Fig. 3g). Notably, photoswitching was fully reversible and compounds remained chemically stable even under prolonged (>12 h) pulsed irradiations with 390 and 450 nm light (Figs. 3b and Fig. S3).

Since membrane-permeant actin inhibitors are potent cytotoxins,[12] the **optojasps** were evaluated *in cellulo* for light-dependent cytotoxic activity in HeLa cells (Fig. 3 and Fig. S1). Multi-LED arrays (DISCO system)[23] were used to deliver pulsed illuminations at different wavelengths. Notably, all **optojasps** were bioactive, indicating that the azo-extension of the parent compound does neither compromise cell permeation nor compound binding. Compared to the dark-state *trans* isomers, most **optojasps** gained potency upon illumination with 390 nm (*cis*-form predominating; Fig. 3g), while some stayed equipotent (**optojasp-2** and **6**). By contrast, the potency of **optojasps-3** and **4** was higher in the dark (*trans*).

To investigate the mode of action and the selectivity of **optojasps** we investigated their effect on the cellular actin cytoskeleton by fluorescence microscopy (Fig. 4). We observed that **optojasps** caused a light-dependent increase of actin nucleation, resulting in formation of large aggregates, and leading to very similar cellular phenotypes as caused by the F-actin stabilizers **1-3**. HeLa cells exposed to the *cis*-active **optojasp-1** showed induction of actin polymerisation into amorphous clumps under 390 nm illumination, while cells maintained in the dark showed no abnormalities in the F-actin network. In line with the photophysical data, the *trans*-active **optojasp-3** displayed an inverted light-dependency with actin cytoskeleton disruption occurring in the dark and with no effect on the organisation of the F-actin network under 390 nm illumination (Fig. 4a). By contrast, the microtubule network was clearly not affected by **optojasp-1** treatment (Fig. 4b), even though the trimethoxy azobenzene motif is found in microtubule-disrupting photostatin photoswitches[23] and resembles a substructure motif of the tubulin-polymerization inhibitors colchicine an combretastatin A4.[28] Our data show that by extending the **optojasp** switches at the combretastatin-like B-ring in *para*,

affinity for tubulin is abrogated and actin-selective conjugates for cytoskeleton disruption are obtained.

Incubation under actin-nucleating illumination conditions (**optojasp-1** with 390 nm light pulses over 5 hours) led to a hyper-aggregated actin cytoskeleton (Fig. 4c). Subsequent irradiation with light that promotes back-isomerization (475 nm pulse block for 1 hour) followed by incubation in the dark for 10 h to further promote back-isomerization phenotypically recovered the regular actin cytoskeleton structure (Fig 4c).

In order to study whether the observed activities were connected to non-specific interactions, we studied the physicochemical properties of the best candidate **optojasp-1** as well as its activity on target. Compound solubility remained unaffected by irradiation, i.e. both *trans*- and *cis*-form of optojasp-1 were equally soluble. Furthermore, by collecting light scattering data at 800 nm wavelength, we could not find any indication for compound aggregation in either *cis*- or *trans*-configuration (see SI for details).

On-target activity was then studied by measuring the rate of F-actin polymerization induced by **optojasp-1**, depending on its configurational state, using pyrene-labeled actin (Fig. 5).[31] We found that both forms of **optojasp-1** stimulated F-actin polymerization, but to a lesser extent as jasplakinolide. Furthermore, the *cis*-form of **optojasp-1** was found significantly more active than the *trans*-form, in good agreement with the cytotoxicity data.

By contrast, the azobenzene extensions **16** or **17** (not shown) devoid of the actin- binding ligand were incapable of promoting F-actin polymerization and did not modify the activity of jasplakinolide, neither in *cis* nor in *trans* form (see ESI). These data strongly suggest that it is the direct molecular interaction of the **optojasps** with the F-actin target that accounts for their properties.

With target selectivity and reversibility established, we evaluated the potential of **optojasps** for photocontrol of cellular dynamics. Actin reorganisation is involved in neuronal development and plasticity,[32] cell cycle and division,[19] as well as cell motility, invasive migration,[18] and endocytosis.[33] When studying cell morphology, we observed that upon irradiation with 390 nm, **optojasp-1** caused cells to detach rapidly from their substrate at doses that caused no morphological changes in the dark (Fig. 6a, movies 1-2). Motile cells exposed to **optojasp-1** immediately stopped migrating upon illumination with 390 nm, reduced lamellipodia formation, and finally rounded up. We then performed cell tracking experiments to quantify the control of cell motility by photoswitching **optojasps**. In line with the phenotypic observations, cell velocity and migration distance was found significantly reduced in a dose dependent manner upon activation with 390 nm light. *Cis*-active **optojasps** were particularly robust in this application, reducing motility threefold in light-targeted cells only minutes after illumination, at doses where cells remained unaffected in the dark (Fig. 6b, movies 3-4).

We also examined whether optojasps could optically control cell division, since its successful completion relies on proper chromosome segregation and correct functionality of the actin contractile ring.[5,19] At intermediate doses **optojasp-1** was indeed capable of

controlling the completion of cell division. While cell division proceeded with chromosome segregation to the state of daughter cell constriction, photoswitching stalled the separation of daughter cells.

This blockade finally resulted in their re-fusion into tetraploids, strongly indicative of a dysfunctional contractile ring (Fig. 6c, movies 5-6). These phenotypic data independently confirm that tubulin assembly remains unaffected by optojasps, which exert selective activity on F-actin dynamics only.

Furthermore, we investigated the ability of the optojasps to optically control processes acutely coupled to cytoskeletal signaling.[34] The myocardin-related transcription factor A (MRTF-A) was selected as an example, as it directly communicates changes of cytoplasmic actin dynamics to gene regulation.[35] G- actin bound MRTF-A is released when F-actin is formed. Liberated MRTF-A translocates into the nucleus where it activates target genes depending on serum response factor (SRF).[36] We first used a fluorescent MRTF-A fusion protein in order to monitor its cellular localization. Indeed, upon treatment with activated optojasps, MRTF-A localized to the nucleus, just as observed after treatment with jasplakinolide. We selected **optojasp-5** for quantitative analysis as this compound has a spontaneous *cis-trans* relaxation rate in the order of the biological response (18 min, Fig. 3) and only a marginally lower efficacy compared to the slowly relaxing **optojasps 1–4**. Without illumination, labelled MRTF-A remained homogenously distributed in the cytoplasm (Fig. 7a). When cells were exposed to **optojasp-5** and to 390 nm light, nuclear translocation of MRTF was significantly enhanced when compared to non-illuminated cells (Fig. 7a). The effect was most prominent at intermediate concentrations (250–750 nM).

Quantification of the nuclear fraction of MRTF-A confirmed the significance of these data (Fig. 7b). These results indicate that MRTF-A can be specifically activated by **optojasp** photocontrol, further validating F-actin assembly as the direct **optojasp** target.

In addition, we studied the function of MRTF-A induction by using a luciferase reporter gene regulated by SRF. Cells treated with **optojasp-5** fully induced reporter gene expression, with strong optical control in the medium concentration range (Fig. 7c). Jasplakinolide-treated control cells carrying the same reporter displayed strong, but illumination-independent induction of luciferase activity upon compound treatment.

Finally, we investigated **optojasps'** ability to exert both time- and cell- specific control over actin-dependent processes *in cellulo*. After delivering illumination bursts to regions of interest (ROIs) comprising single selected cells within a cell population, cellular response was individually monitored. For this experiment the slowly relaxing **optojasp-1** worked again well (Fig. 8, Movies 7-8). We reproducibly observed that light activation triggered actin-dependent MRTF-A translocation to the nucleus in exactly the defined ROI, with cell-by-cell spatial control applied side-by-side. The response that was both stable and rapid, and cross-talk to neighbouring cells was not observed. In non-illuminated cells, MRTF-A remained in the cytosol. Recovery was not evident on the timescale of the experiment, probably because stimulated F-actin aggregation needs longer time to recover (cmp. Fig. 4c). Nevertheless, these data strongly suggest that optojasps directly work on F-actin as target

and are capable of acutely blocking actin dynamics on the minute timescale with high spatial precision.

Taken together, our data show that **optojasps** are a robust and powerful tool to optically control the actin cytoskeleton and processes that depend on it. They can be used non-invasively in live cells, with exquisite spatial and temporal precision at the cellular level, and enable optical control over actin nucleation and cytotoxicity in cells, as well as over cell motility and cytoskeletal signalling.

Discussion

Optical control of biological activity by using caged compounds, optogenetics, and more recently photopharmacology, has advanced significantly in recent years. Photouncaging is by now routinely applied for spatiotemporal control in biology, particularly in neuroscience where caged neurotransmitters are standard tools.[37] However, to our knowledge, reversibly controllable actin modulators have not yet been introduced for biological studies.

Precision control of cytoskeleton-associated proteins with light has been recently demonstrated by using optogenetics involving proteins that indirectly act on the actin cytoskeleton.[38–40] Engineering actin itself has been rather difficult due to the strong influence even small modifications have on its proper functioning. On the other hand, small molecule photoswitches for the direct optical control of the microtubule cytoskeleton by tubulin polymerization inhibition have been developed[23,41] and have already led to applications in neuroscience, morphogenesis and *in vivo* applications in embryology.[42–44] Photoswitchable tubulin stabilisers were recently reported as well.[45] By analogy, we expect that the small molecule **optojasps** introduced here as photoswitchable F-actin modulators will provide a powerful tool for studying actin biology in a spatiotemporally controlled manner. In particular, we surmise that the ability to easily photo-tune the inhibitory activity of the **optojasps** by varying the wavelength of illumination (“photodosing”, Fig. 3) to sensitively set the isomer ratio above or below its activity threshold offers a robust and adaptable method for complex biological experiments, which is particularly advantageous when compared to irreversible photouncaging approaches.

Optojasps retain most of the potency of the parent compound jasplakinolide and can be expected to bind to the same binding site on F-actin, considering all functional and phenotypic data acquired. However, the discovery of both *cis*-active and *trans*-active compounds alongside with compounds with barely photoswitchable bioactivity is intriguing considering their rather similar chemical structures. It suggests a specific molecular interaction of the **optojasps** with their target that directly involves the configurationally bistable azobenzene.

The **optojasp** design is based on an azo-extension of the jasplakinolide structural scaffold. Recent structure elucidations of F-actin bound with jasplakinolide and its Lys analog by using cryo-electron microscopy showed that both bind at regular intervals inside the F-actin filament contacting three adjacent actin subunits.[46,47] They reinforce the fiber by stabilizing a state of partial ATP hydrolysis that is only transient during regular F-actin turnover.[47]

Interestingly, the lysine side chain of the bound analogue projects toward the interior of F-actin and extends into an inner cavity of moderate volume that is open to the outside (see Figure S2).

The macrocycle's binding pose can be expected to be retained for jasplakinolide conjugates. The azo-extension will then interact with the interior of cavity and affect the affinity of the **optojasps** to F-actin. As the space in this cavity is confined, the ability to stabilize the F-actin fibre would become dependent on switch topology and its configuration. Such a model could tentatively explain the "switchability" and the ability to generate "*cis*-active" (**optojasp-1**) and "*trans*- active" modulators (**optojasp-3**), which would result from the individually different optojasp topologies and conformational preferences. Furthermore, altered conformational preferences of the **optojasp** macrocycle could contribute to "switchability" as well.

By contrast, changes in general compound properties are likely not strongly contributing to compound activity. Our experiments showed that solubility does not depend on switch configuration, neither was aggregation observed. While not investigated for all optojasps in detail, the single cell irradiation experiments conducted for studying MRTF-A signalling (Fig. 8) as well as experiments with pre-irradiated compounds (data not shown) indicated that both the active and the inactive state should have comparable cell permeability. If this wasn't the case, local concentration reached by irradiation would probably be insufficient for observing any compound activity localized in the extremely small volume of a single cell (approx. 10^{-14} m^3). Furthermore, "spilling" of activity to neighbouring cells, indicative of a highly diffusible active state populated by irradiation, has also not been observed during these experiments. Finally, if the azobenzene configuration (*cis* or *trans*) would generally affect cell permeability, a concordant activity profile for all optojasps should emerge *in cellulo* – which is not the case. Together with the F-actin polymerization experiment, which supported direct on-target activity, these data strongly suggest that a direct structural interaction of the switch with the binding cavity is likely eliciting the observed properties.

Conclusion

Further mechanistic characterization and functional optimization notwithstanding, we expect that **optojasps** will become highly useful research tools for deciphering the complex role of actin in cell biology with the high temporal and spatial resolution that only light can provide. Importantly, our experimentation showed that switching the activity of the optojasps results in highly localized, acute activity on F-actin. This activity can be confined to a single cell. Since actin is highly conserved among all eukaryotes, the **optojasps** should be applicable in a variety of cell types originating from different organisms, provided they can be illuminated appropriately. Lastly, the **optojasps**' ability to inhibit actin dynamics only in selected cells could open new vistas for functional research in cancer biology and neuronal regeneration. **Optojasps** should hence prove a versatile and powerful tool for enabling high-precision cytoskeletal control inaccessible to other methods.

Supplementary Material

Refer to Web version on PubMed Central for supplementary material.

Acknowledgement

This research was supported by the National Institutes of Health (R01 GM126228 to D.T.), the Deutsche Forschungsgemeinschaft (SFB1032 to D.T., O.T.-S. and S.Z.; SFB152 and Emmy Noether grant to O.T.-S.), and the TMWWDG (equipment grant No. 43–5572-321–12040-12 to H.-D.A.). H.-D. A. is a PI in the DFG-funded cluster of excellence “Balance of the microverse” (EXS 2051). M.B. was supported by LMU-Excellent (postdoctoral fellowship), V.N. by the DAAD (predoctoral fellowship), and S.P. by the GDCh (Hofmann-fellowship). We thank M. Reynders for help with synthesis and discussions, L. de la Rosa for help with cell biology, A. Akhmanova (Utrecht University, NL) for donating mCherry-Lifeact MDA-MB-231 cells, and the microscopy platform CALM for imaging support.

References

(1). Pollard TD; Borisy GG, Cellular Motility Driven by Assembly and Disassembly of Actin Filaments. Cell 2003, 112, 453–465. [PubMed: 12600310]

(2). Dominguez R; Holmes KC, Actin Structure and Function. Ann. Rev. Biophys 2011, 40, 169–186. [PubMed: 21314430]

(3). Papandreou M-J; Leterrier C. The Functional Architecture of Axonal Actin. Mol. Cell. Neurosci 2018, 91, 151–159. [PubMed: 29758267]

(4). Eustermann S; Schall K; Kostrewa D; Lakomek K; Strauss M; Moldt M; Hopfner K-P, Structural Basis for ATP-dependent Chromatin Remodelling by the INO80 Complex. Nature 2018, 556, 386–390.

(5). Glotzer M, The Molecular Requirements for Cytokinesis. Science 2005, 307, 1735–1739. [PubMed: 15774750]

(6). Allingham JS; Klenchin V; Rayment AI, Actin-Targeting Natural Products: Structures, Properties and Mechanisms of Action. Cell. Mol. Life Sci 2006, 63, 2119–2134. [PubMed: 16909206]

(7). Katagiri K; Matsuura S, Antitumor Activity of Gytoghalasin D. J. Antibiot 1971, 24, 722–723.

(8). Spector I; Shochet NR; Kashman Y; Groweiss A, Latrunculins: Novel Marine Toxins That Disrupt Microfilament Organization in Cultured Cells. Science 1983, 219, 493. [PubMed: 6681676]

(9). Bubb MR; Senderowicz AM; Sausville EA; Duncan KL; Korn ED, Jasplakinolide, a Cytotoxic Natural Product, Induces Actin Polymerization and Competitively Inhibits the Binding of Phalloidin to F-Actin. J. Biol. Chem 1994, 269, 14869–14871. [PubMed: 8195116]

(10). Holzinger A; Blaas K, In Cytoskeleton Methods and Protocols: Methods and Protocols, (Ed. Gavin RH), Springer New York, New York, NY, 2016, pp. 243–261.

(11). Holzinger A, In Cytoskeleton Methods and Protocols, (Ed. Gavin RH), Humana Press, Totowa, NJ, 2010, pp. 71–87.

(12). Fenteany G; Zhu S, Small-Molecule Inhibitors of Actin Dynamics and Cell Motility. Curr. Top. Med. Chem 2003, 3, 593–616. [PubMed: 12570855]

(13). Peterson JR; Mitchison TJ, Small Molecules, Big Impact: a History of Chemical Inhibitors and the Cytoskeleton. Chem. Biol 2002, 9, 1275–1285. [PubMed: 12498880]

(14). Melak M; Plessner M; Grosse R, Actin Visualization at a Glance. J. Cell. Sci 2017, 130, 525–530. [PubMed: 28082420]

(15). Lukinavicius G; Reymond L; D’Este E; Masharina A; Gottfert F; Ta H; Guther A; Fournier M; Rizzo S; Waldmann H; Blaukopf C; Sommer C; Gerlich DW; Arndt H-D; Hell SW; Johnsson K, Fluorogenic Probes for Live-Cell Imaging of the Cytoskeleton. Nat. Methods 2014, 11, 731–733. [PubMed: 24859753]

(16). Milroy L-G; Rizzo S; Calderon A; Ellinger B; Erdmann S; Mondry J; Verveer P; Bastiaens P; Waldmann H; Dehmelt L; Arndt H-D, Selective Chemical Imaging of Static Actin in Live Cells. J. Am. Chem. Soc 2012, 134, 8480–8486. [PubMed: 22475347]

(17). Stehn JR; N. Haass K; Bonello T; Desouza M; Kottyan G; Treutlein H; Zeng J; Nascimento PRBB; Sequeira VB; Butler TL; Allanson M; Fath T; Hill TA; McCluskey A; Schevzov G; Palmer SJ; Hardeman EC; Winlaw D; V. Reeve E; Dixon I; Weninger W; Cripe TP; Gunning PW, A Novel Class of Anticancer Compounds Targets the Actin Cytoskeleton in Tumor Cells. Cancer Res. 2013, 73, 5169–5182. [PubMed: 23946473]

(18). Blanchoin L; Boujemaa-Paterski R; Sykes C; Plastino J, Actin Dynamics, Architecture, and Mechanics in Cell Motility. Physiol. Rev 2014, 94, 235–263. [PubMed: 24382887]

(19). Heng Y-W; Koh C-G, Actin Cytoskeleton Dynamics and the Cell Division Cycle. Int. J. Biochem. Cell Biol 2010, 42, 1622–1633. [PubMed: 20412868]

(20). Broichhagen J; Frank JA; Trauner D, A Roadmap to Success in Photopharmacology. Acc. Chem. Res 2015, 48, 1947–1960. [PubMed: 26103428]

(21). Velema WA; Szymanski W; Feringa BL, Photopharmacology: Beyond Proof of Principle J. Am. Chem. Soc 2014, 136, 2178–2191. [PubMed: 24456115]

(22). Pittolo S; Gómez-Santacana X; Eckelt K; Rovira X; Dalton J; Goudet C; Pin J-P; Llobet A; Giraldo J; Llebaria A; Gorostiza P, An Allosteric Modulator to Control Endogenous G Protein-Coupled Receptors with Light. Nat. Chem. Biol 2014, 10, 813–815. [PubMed: 25173999]

(23). Borowiak M; Nahaboo W; Reynders M; Nekolla K; Jalinot P; Hasserodt J; Rehberg M; Delattre M; Zahler S; Vollmar A; Trauner D; Thorn-Seshold O, Photoswitchable Inhibitors of Microtubule Dynamics Optically Control Mitosis and Cell Death. Cell 2015, 162, 403–411. [PubMed: 26165941]

(24). Hüll K; Morstein J; Trauner D, In Vivo Photopharmacology. Chem. Rev 2018, 118, 10710–10747. [PubMed: 29985590]

(25). Beharry AA; Wooley GA, Azobenzene Photoswitches for Biomolecules: Chem. Soc. Rev 2011, 40, 4422–4437 [PubMed: 21483974]

(26). Schönberger M; Althaus M; Fronius M; Clauss W; Trauner D, Controlling Epithelial Sodium Channels with Light Using Photoswitchable Amilorides. Nat. Chem 2014, 6, 712. [PubMed: 25054942]

(27). Wegener M; Hansen MJ; Driessen AJM; Szymanski W; Feringa BL, Photocontrol of Antibacterial Activity: Shifting from UV to Red Light Activation. J. Am. Chem. Soc 2017, 139, 17979–17986. [PubMed: 29136373]

(28). Tron GC; Pirali T; Sorba G; Pagliai F; Busacca S; Genazzani AA, Medicinal Chemistry of Combretastatin A4: Present and Future Directions. J. Med. Chem 2006, 49, 3033–3044. [PubMed: 16722619]

(29). Gaspari R; Prota AE; Bargsten K; Cavalli A; Steinmetz MO, Structural Basis of cis- and trans-Combretastatin Binding to Tubulin. Chem 2017, 2, 102–113.

(30). Tannert R; Hu T-S; Arndt H-D; Waldmann H, Solid-Phase Based Total Synthesis of Jasplakinolide by Ring-Closing Metathesis Chem. Commun 2009, 1493–1495.

(31). Doolittle LA; Rosen MK; Padrick SB, Measurement and Analysis of in vitro Actin Polymerization. Methods Mol. Biol 2013, 1046, 273–293. [PubMed: 23868594]

(32). Kevenaar JT; Hoogenraad CC, The Axonal Cytoskeleton: From Organization to Function. Front. Mol. Neurosci 2015, 8, 44. [PubMed: 26321907]

(33). Mooren OL; Galetta BJ; Cooper JA, Roles for Actin Assembly in Endocytosis. Annu. Rev. Biochem 2012, 81, 661–686. [PubMed: 22663081]

(34). Gegenfurter FA; Zsisis T; Al Dadaf N; Schrimpf W; Kliesmete Z; Ziegenhain C; Enard W; Kazmaier U; Lamb DC; Vollmar AM; Zahler S, Transcriptional Effects of Actin-Binding Compounds: The Cytoplasm Sets the Tone. Cell. Mol. Life Sci 2018, 75, 4539–4555. [PubMed: 30206640]

(35). Olsen EN; Nordheim A, Linking Actin Dynamics and Gene Transcription to Drive Cellular Motile Functions. Nat. Rev. Cell Biol 2010, 11, 353–365.

(36). Parmacek MS, Myocardin-Related Transcription Factors Circul. Res 2007, 100, 633–644.

(37). Ellis-Davies GCR, Caged Compounds: Photorelease Technology for Control of Cellular Chemistry and Physiology. Nat. Methods 2007, 4, 619–628. [PubMed: 17664946]

(38). Wu YI; Frey D; Lungu OI; Jaehrig A; Schlichting I; Kuhlman B; Hahn KM, A Genetically Encoded Photoactivatable Rac Controls the Motility of Living Cells. Nature 2009, 461, 104–108. [PubMed: 19693014]

(39). Valon L; Marín-Llauradó A; Wyatt T; Charras G; Trepat X, Optogenetic Control of Cellular Forces and Mechanotransduction. Nat. Commun 2017, 8, 14396. [PubMed: 28186127]

(40). van Haren J; Charafeddine RA; Ettinger A; Wang H; Hahn KM; Wittmann T, Local Control of Intracellular Microtubule Dynamics by EB1 Photodissociation. Nat. Cell Biol 2018, 20, 252–261. [PubMed: 29379139]

(41). Gao L; Kraus Y; Wranik M; Weinert T; Pritzl S; Meiring J; Bingham R; Olieric N; Akhmanova A; Lohmüller T; Steinmetz M; Thorn-Seshold O, Photoswitchable Microtubule Inhibitors Enabling Robust, GFP-Orthogonal Optical Control Over the Tubulin Cytoskeleton. submitted, preprint at bioRxiv 2019.07.27, 10.1101/716233.

(42). Singh A; Saha T; Begemann I; Ricker A; Nüsse H; Thorn-Seshold O; Klingauf JR; Galic M; Matis M, Polarized Microtubule Dynamics Directs Cell Mechanics and Coordinates Forces During Epithelial Morphogenesis. Nat. Cell Biol 2018, 20, 1126–1133. [PubMed: 30202051]

(43). Zenker J; White MD; Templin RM; Parton RG; Thorn-Seshold O; Bissiere S; Plachta NA, Microtubule-Organizing Center Directing Intracellular Transport in the Early Mouse Embryo: Science 2017, 357, 925–928. [PubMed: 28860385]

(44). Eguchi K; Taoufiq Z; Thorn-Seshold O; Trauner D; Hasegawa M; Takahashi T, Wild-Type Monomeric α-Synuclein Can Impair Vesicle Endocytosis and Synaptic Fidelity via Tubulin Polymerization at the Calyx of Held. J. Neurosci 2017, 37, 6043–6052. [PubMed: 28576942]

(45). Müller-Deku A; Loy K; Kraus Y; Heise C; Bingham R; Ahlfeld J; Trauner D; Thorn-Seshold O, Photoswitchable Microtubule Stabilisers Optically Control Tubulin Cytoskeleton Structure and Function. submitted, preprint at bioRxiv 2019.09.22, 10.1101/778993.

(46). Pospich S; Kumpula E-P; von der Ecken J; Vahokoski J; Kursula I; Raunser S, Near-Atomic Structure of Jasplakinolide-Stabilized Malaria Parasite F-Actin Rveals the Structural Basis of Filament Instability. Proc. Natl. Acad. Sci. U. S. A 2017, 114, 10636–10641. [PubMed: 28923924]

(47). Merino F; Pospich S; Funk J; Wagner T; Küllmer F; Arndt H-D; Bieling P; Raunser S, Structural Transitions of F-Actin Upon ATP Hydrolysis at Near-Atomic Resolution Revealed by Cryo-EM. Nat. Struct. Mol. Biol 2018, 25, 528–537. [PubMed: 29867215]

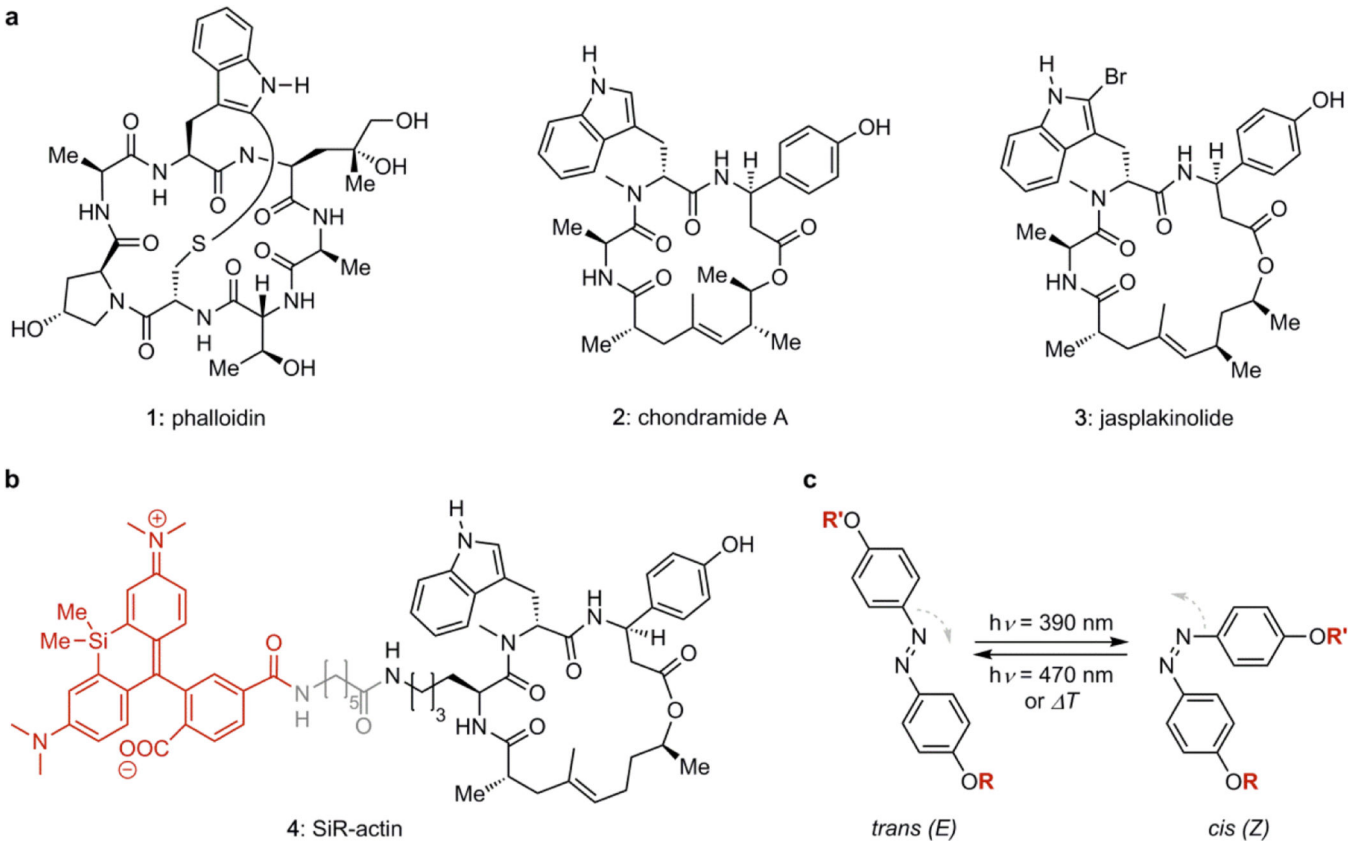

Figure 1.

(a) Chemical structures of F-actin stabilizing natural products. (b) Structure of SiR-actin composed of the silico-rhodamine fluorophore (red), a linker (grey), and the optimized jasplakinolide scaffold (right). (c) Azobenzene isomerization controlled by illumination.

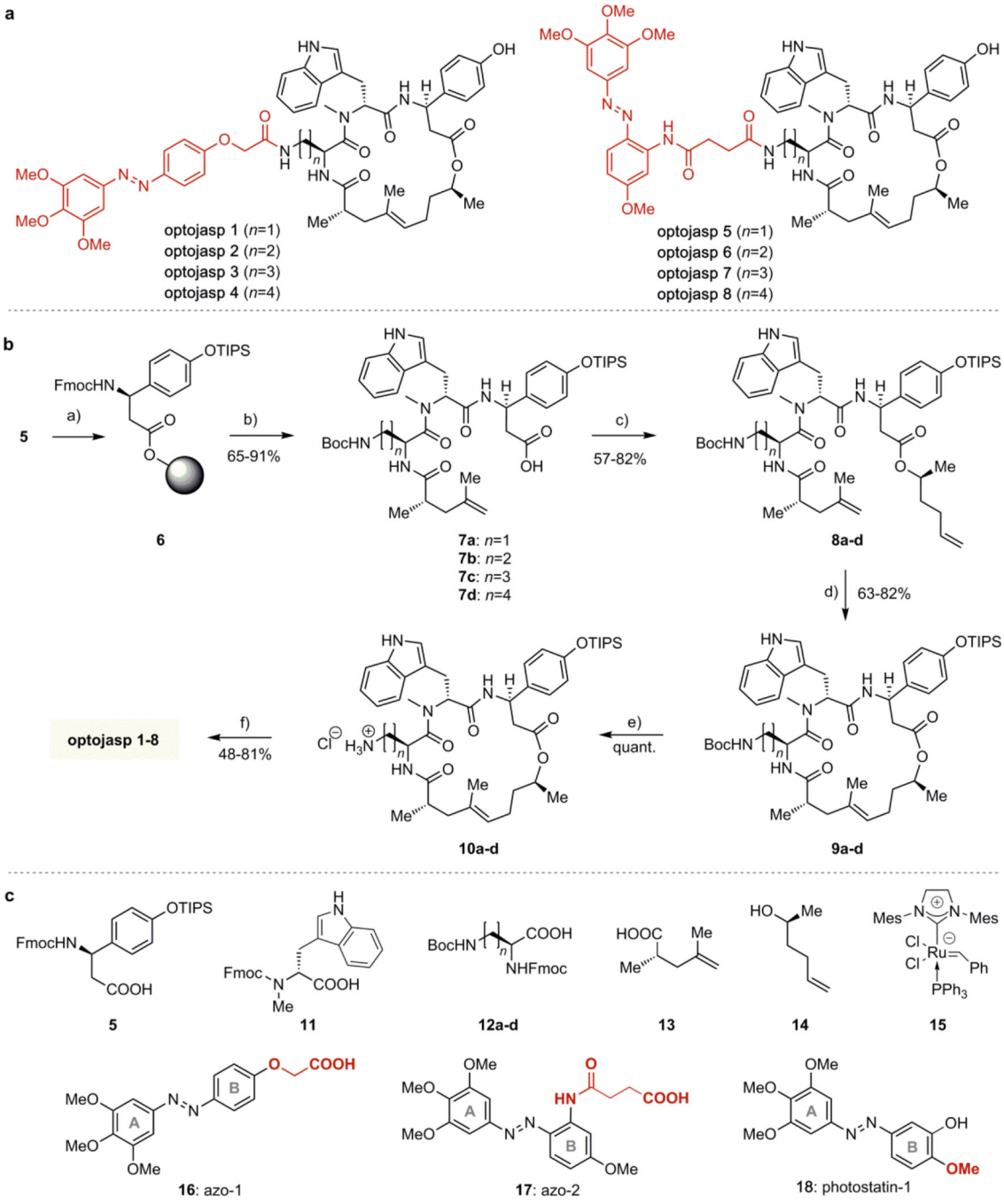

Figure 2.

(a) Structures of **optojasps 1** - **8**. (b) Chemical synthesis of optojasps. Conditions: a) 2-Chlorotrityl chloride resin, DIPEA, CH_2Cl_2/DMF; b) 1. piperidine, DMF; 2. HATU, HOAt, **2**, DIPEA, CH_2Cl_2/DMF; 3. piperidine, DMF; 4. HATU, HOAt, **12a** or **b** or **c** or **d**, DIPEA, CH_2Cl_2/DMF; 5. piperidine, DMF; 6. HATU, HOAt, **4**, DIPEA, CH_2Cl_2/DMF; 7. HFIP, CH_2Cl_2; c) EDCI, DMAP, DIPEA, **5**, CH_2Cl_2/DMF; d) catalyst **15**, CH_2Cl_2, rfx.; e) 4M HCl in dioxane, CH_2Cl_2, 0 °C; f) 1. **16** or **17**, HATU, DIPEA, THF; 2. HF-pyridine, THF. (c)

Building blocks used for **optojasp** synthesis and structure of tubulin-selective photostatin-1 (**18**). See text and Supporting Information for details.

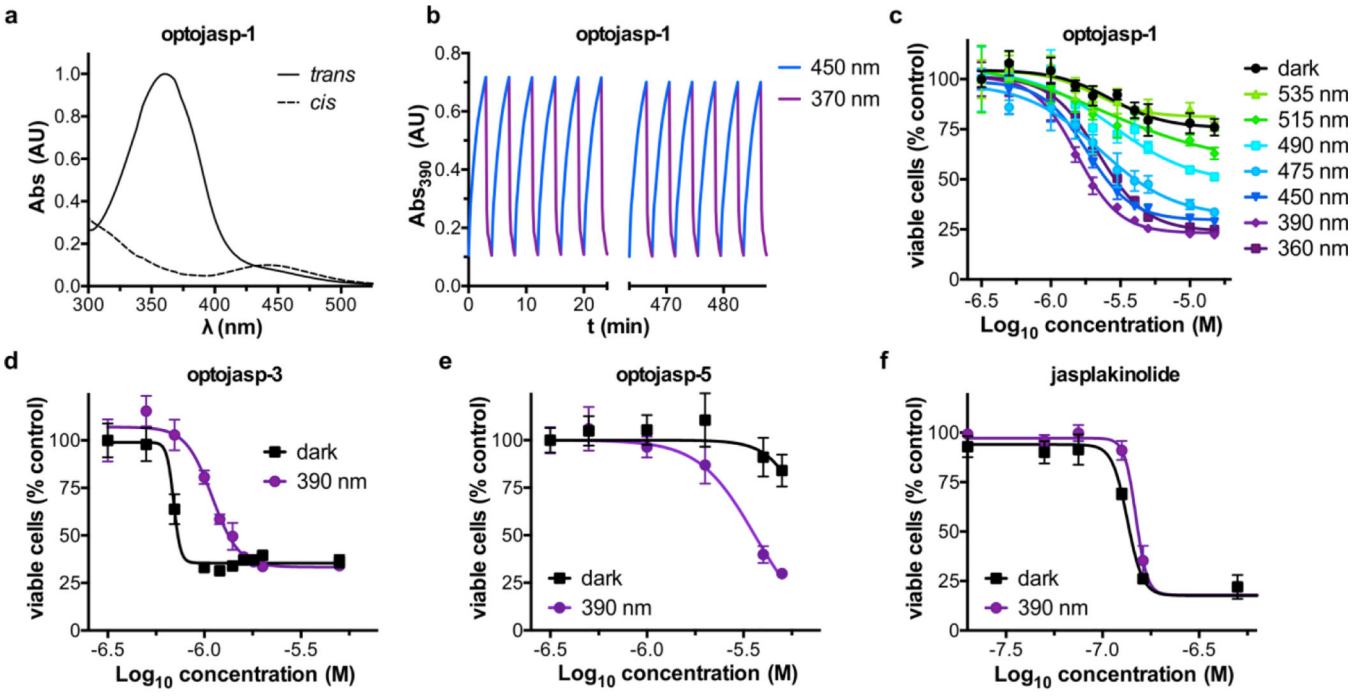

g

Compound	λ (max) (*E*)	λ (max) (*Z*)	$t_{1/2}$ (25 °C) in MeCN	$t_{1/2}$ (37 °C) in PBS	EC_{50} (*E*) (μM)	EC_{50} (*Z*) (μM)
optojasp-1	361 nm	438 nm	36 h	262 min	> 15	1.5
optojasp-2	361 nm	441 nm	37 h	256 min	1.7	1.4
optojasp-3	360 nm	339 nm	27 h	191 min	0.7	1.1
optojasp-4	360 nm	442 nm	37 h	267 min	1.2	1.9
optojasp-5	391 nm	452 nm	81 min	18 min	> 5	3.1
optojasp-6	391 nm	453 nm	77 min	17 min	2.0	1.8
optojasp-7	390 nm	453 nm	80 min	17 min	> 4	2.2
optojasp-8	391 nm	452 nm	83 min	18 min	> 10	1.4

h

λ (nm)	EC_{50} (μM)
360	2.2
390	1.5
410	1.6
450	1.8
475	2.4
490	5.8
515	> 15
535	> 15
dark	> 15

Figure 3.

Switching properties and cytotoxicity of **optojasps**. (a) Absorption spectra of *cis* and *trans* **optojasp-1**. (b) Photoswitching reversibility monitored by absorption at 390 nM on pulsed treatment with 390 nm and 450 nm light. (c) Wavelength-dependent cytotoxicity of **optojasp-1** determined by MTT assay. (d-f) Photoswitching-dependent cell toxicity profiles for (d) "*trans*- active" **optojasp-3**, (e) "*cis*-active" **optojasp-5**, (f) jasplakinolide (**3**). (g) Photophysical and cytotoxicity parameters for **optojasps-1–8**, see Fig. S1 for details. (h) Wavelength-dependent cytotoxicity of *cis*-active **optojasp-1**, related to panel a. All data were obtained with HeLa cells (45 h, pulsed illuminations of 75 ms every 15 s at the specified wavelength or in the dark).

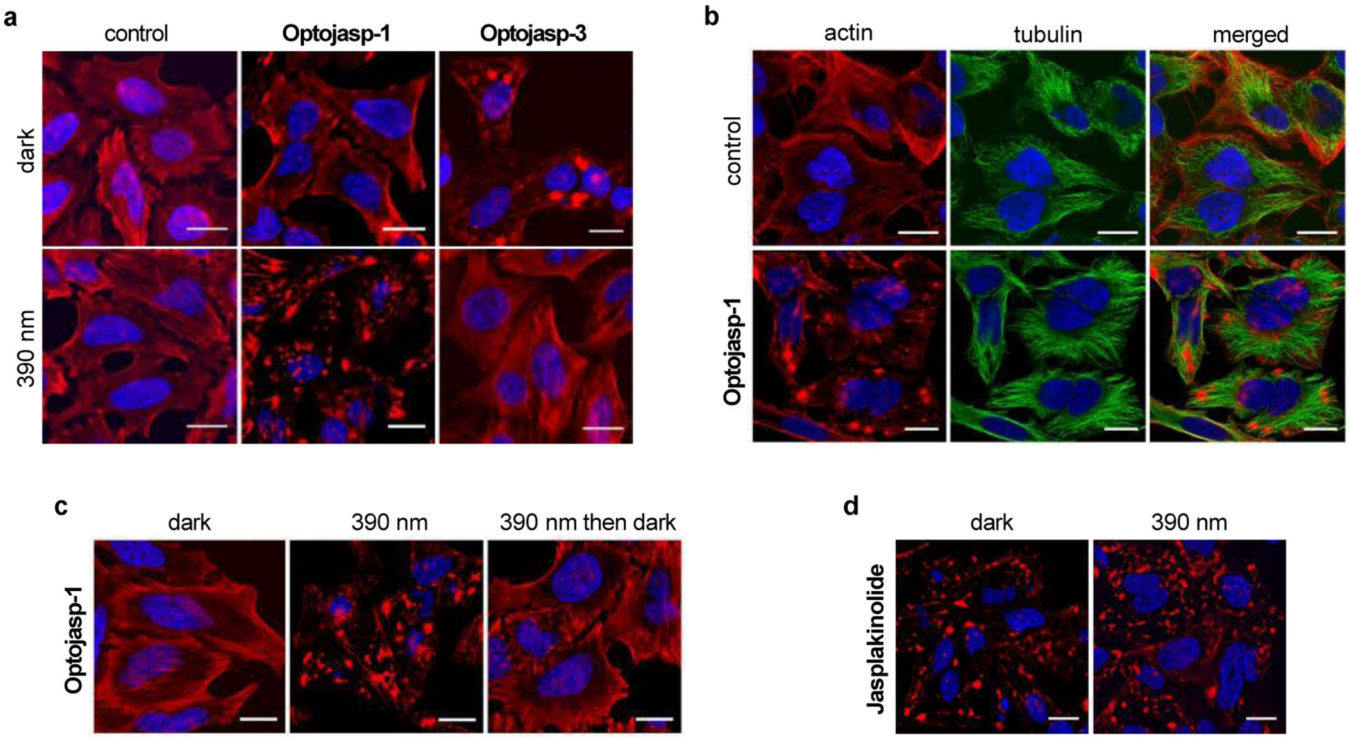

Figure 4.

Light-dependent selective disruption of the actin cytoskeleton by **optojasps**. (a) HeLa cells treated with **optojasps** (1 μM) in the absence or presence of 390 nm illumination, stained for F-actin (red). (b) HeLa cells untreated or treated with **optojasp-1** (1 μM) in the absence or presence of 390 nm illumination, stained for tubulin (green). (c) Cells treated with **optojasp-1** (3 μM) and exposed to 390 nm light for 5 h ("390 nm"), subsequently exposed to 475 nm light for 1 h then kept in darkness for 12 h ("390 nm then dark"). (d) HeLa cells treated with jasplakinolide (**3**, 100 nM) for 5 h in the absence or presence of 390 nm irradiation. Nuclear DNA was stained with Hoechst 33342 (blue), cells were imaged after fixation, scale bar 20 μm.

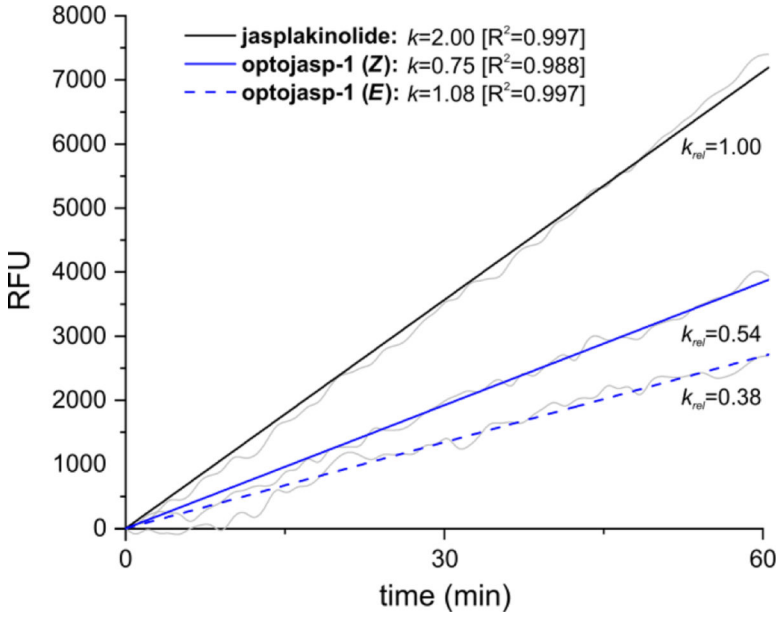

Figure 5.

Illumination dependent capacity of **optojasp-1** for inducing actin-polymerization *in vitro*. ***trans*-optojasp-1**, ***cis*-optojasp-1**, or jasplakinolide (**3,** 20 μM each) were incubated with pyrene-labelled actin (5 μM) under low salt, non-polymerizing conditions.[31] Polymerization was monitored by pyrene fluorescence emission measurement at λ_{Em} = 410 nm after low intensity excitation at λ_{Em} = 350 nm in 60 s intervals over 4 h at 37°C. Optojasp configuration remained stable under these conditions (see Fig. S5). Data are shown for the initial linear phase (1 h). All measurements were performed in duplicates in 384-well plates. RFU: relative fluorescence units, detector response normalized to fluorescence of pyrene-labelled G-actin in non-polymerizing buffer. External fluorophore **16** was added to **3** to correct for azobenzene absorbance; *k*: slopes of linearly fitted curves in RFU/s; k_{rel}: comparative potential for induction of actin polymerization, normalized to jasplakinolide (k_{rel} = 1).

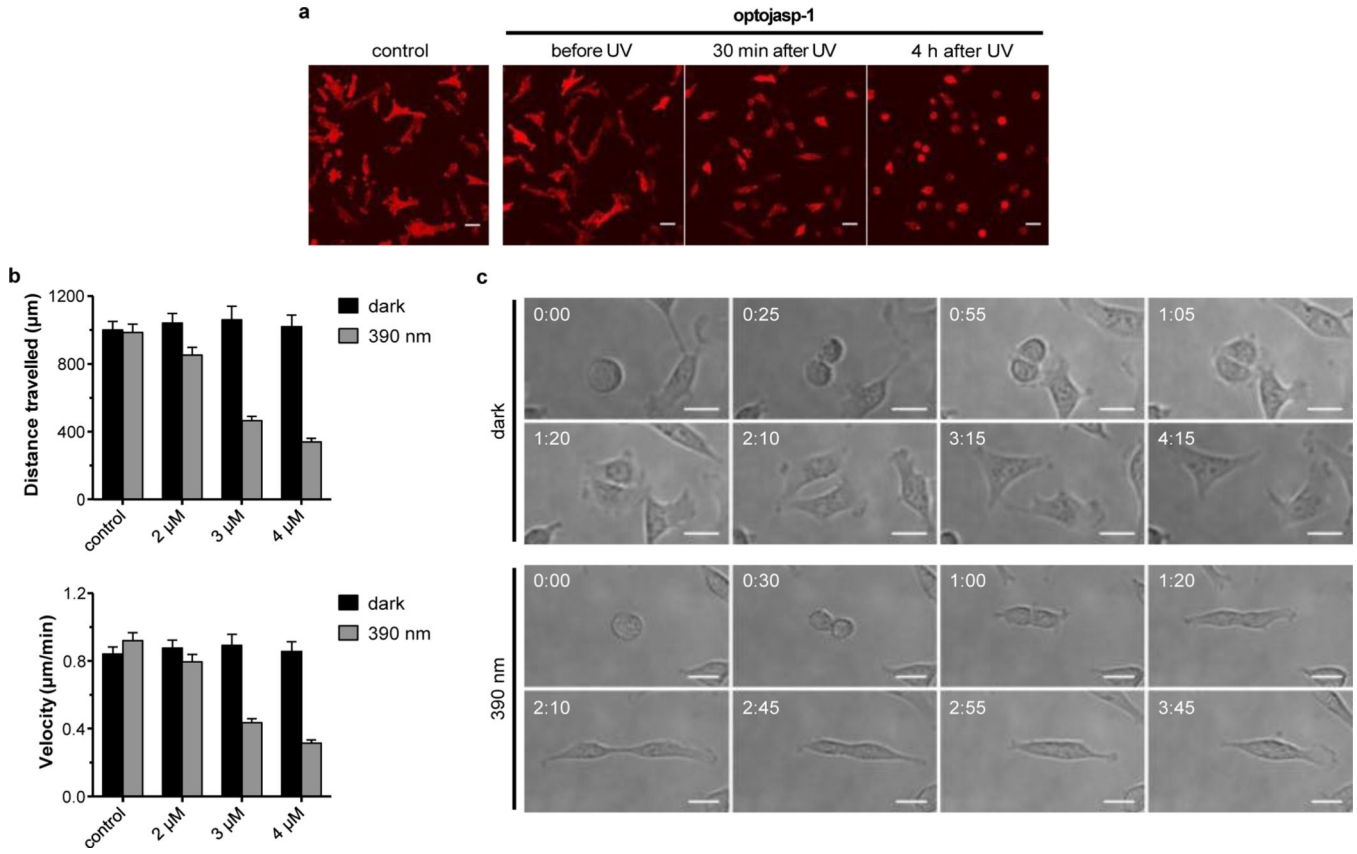

Figure 6.

Optical control over cell shape, motility, and division. (a) Motile cells exposed to **optojasp-1** (5 μM) before and after illumination with 390 nm, see movies 1-2. (b) Quantification of light-dependent cell motility parameters with escalating doses of **optojasp-1**, see movies 3-4.(c) Dividing cells treated with **optojasp-1** (2.5 μM) in the dark or under 390 nm illumination, see movies 5-6). All experiments were conducted using MDA-MB-231 cells stably expressing mCherry- Lifeact; scale bars 40 μm, time shown as hh:mm. See Supporting Info for experimental details.

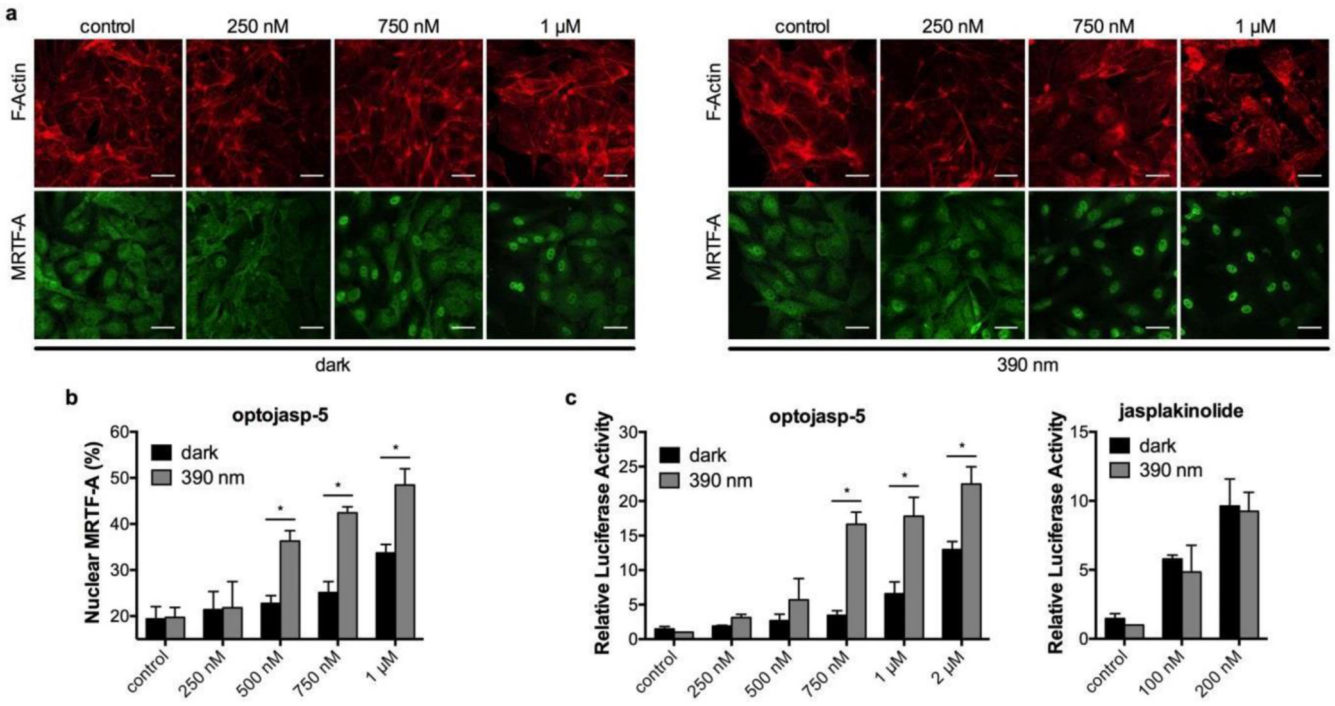

Figure 7.

Optical control over MRTF-A signalling in human umbilical vein endothelial cells (HUVECs). (a) Cells expressing mCherry labelled MRTF-A exposed to escalating doses of **optojasp- 5** in the dark or with 390nm irradiation, stained for F-actin, and imaged after fixation. Scale bars 40 μm. (b) Quantification of the nuclear fraction of MRTF-A. (c) Dual luciferase reporter gene assay for SRF response elements in cells incubated with **optojasp-5** or **jasplakinolide**. Luciferase reporter activity is expressed as firefly RLU normalized to the constitutive control renilla expression level. Bar graph results are given as mean ± SD; statistical significance determined by unpaired Student *t*-test, $p \leq 0.05$. See Supporting Information for details.

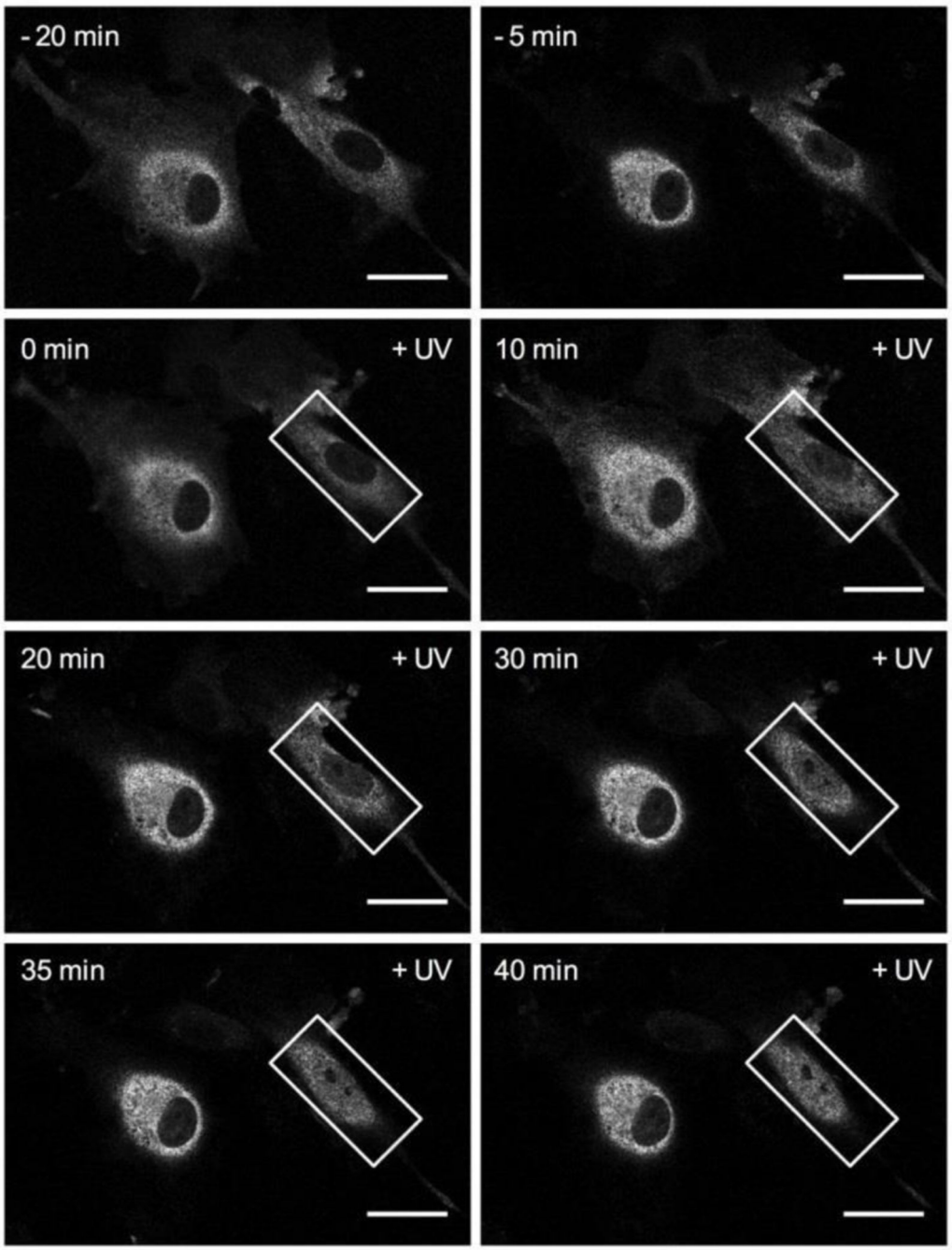

Figure 8.

Time lapse imaging series of MRTF-A:mCherry-expressing HUVEC cells following treatment with 750 nM **optojasp-1** and cell-specific, localized illumination (+UV, white rectangle ROI, 405 nm irradiation). Scale bars 20 μm.